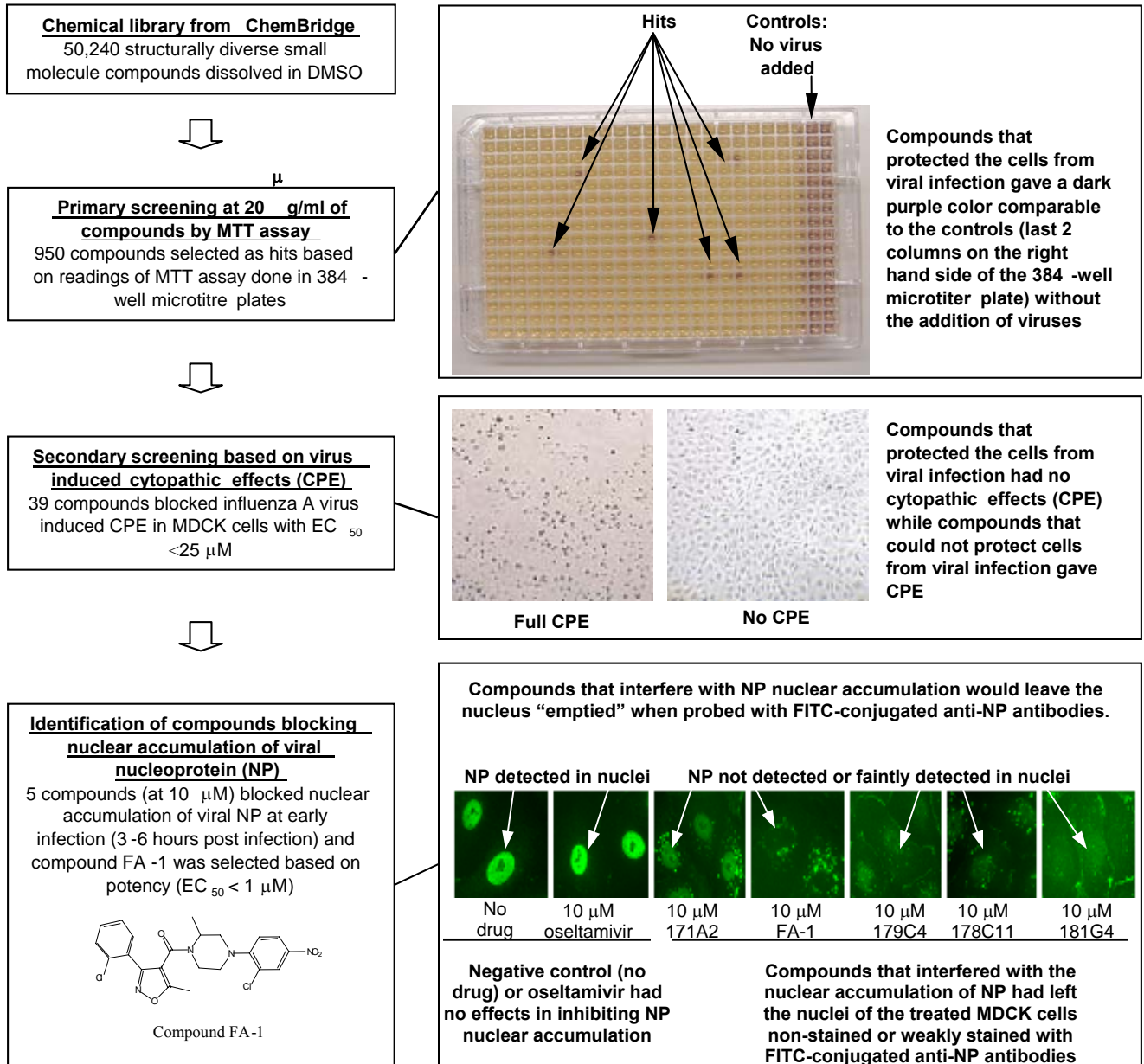


Supplementary materials



Supplementary Fig. 1. Isolation of small-molecule inhibitors of influenza A virus from a phenotype-based screen and identification of compounds that affects the nuclear localization/accumulation of viral nucleoproteins in the infected cells. Shown are the

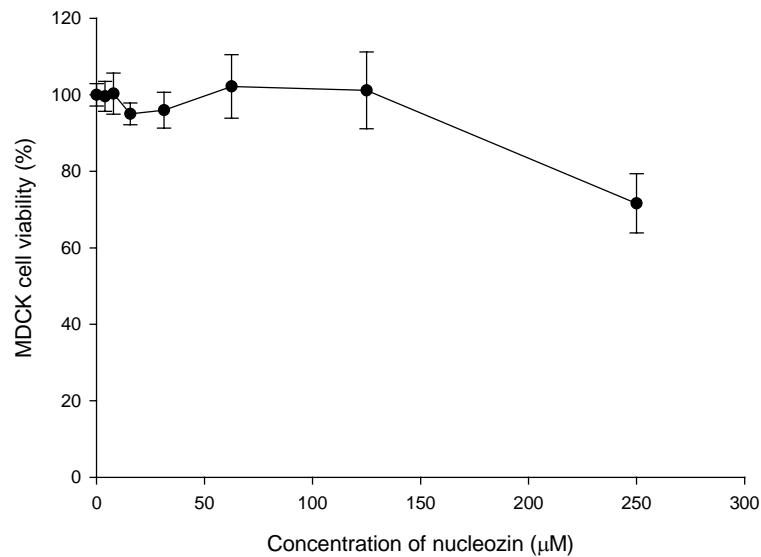
processes and results involved in the selection of a panel of biologically active compounds against the infection of influenza A virus in a MDCK cellular infection model. A representative 384-well microtiter plate used in the HTS and the enlarged images of the MDCK cells are included shown to illustrate the criteria of hit selection.

Using the equation published by Zhang et al:

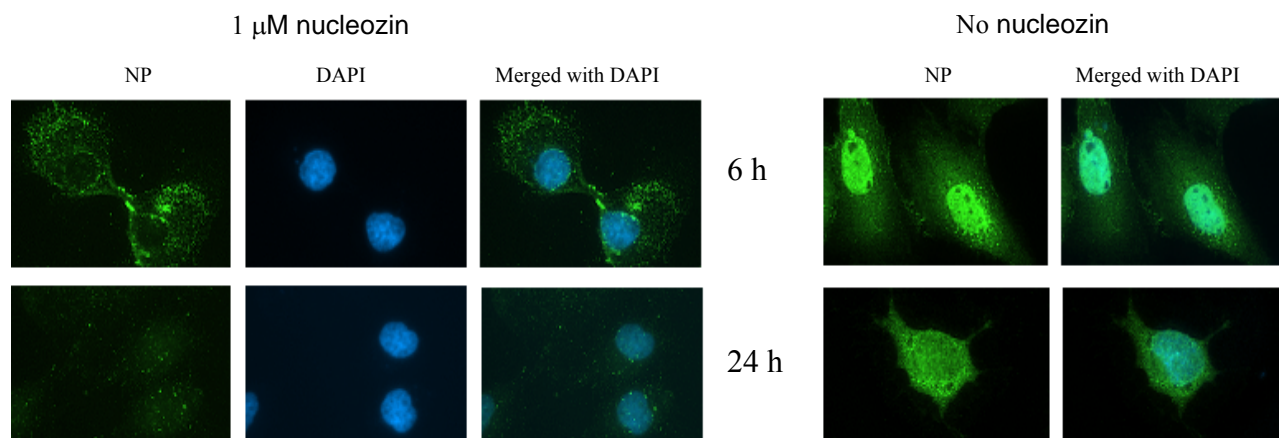
$$\text{Z-factor} = 1 - \frac{3 \times (\sigma_p + \sigma_n)}{|\mu_p - \mu_n|}.$$

Where δ_p = standard deviation of positive controls (no virus added), δ_n = standard deviation of negative controls (100 PFU added per well), μ_p = mean of positive controls (no virus added), μ_n = mean of negative controls (100 PFU added per well).

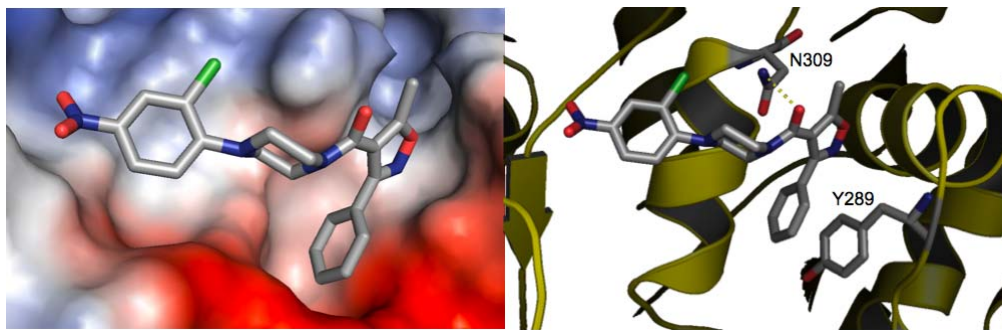
The Z factor of the 384-well formatted MTT assay = 0.58, indicating that the assay is suitable for HTS. We selected only the compounds that had high readings in MTT assays and showed full protection of MDCK cells from virus-induced CPE for further studies. For fluorescence microscopy screen, infected cells were treated with mouse anti-influenza A NP antibodies (conjugated with FITC) in the presence or absence of the compounds (10 μ M) and visualized using a Leica DMIL inverted microscope equipped with DC300F digital imaging system.



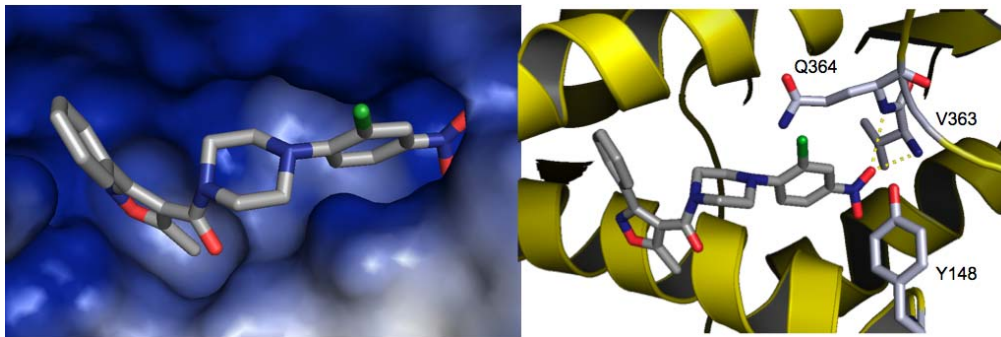
Supplementary Fig. 2. Cytotoxicity evaluation of nucleozin in MDCK cells. The cytotoxicity of nucleozin in MDCK cells was evaluated by MTT assay. A toxic control (1%) SDS was included to ensure the MTT assay was working properly. The highest concentration of nucleozin used was 250 µM due to solubility limitations. SigmaPlot 8.0 (SPSS, IL) was used for graph plotting. Experiments were carried out in triplicate and repeated twice. The mean value is shown with standard deviation.



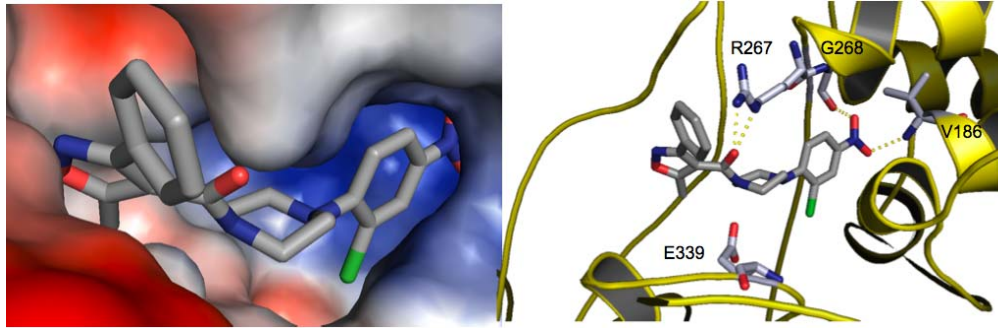
Supplementary Fig. 3. Nucleozin blocked nuclear accumulation of influenza A NP in virus-infected MDCK cells. Cells were infected with A/WSN/33 virus (5 MOI) in the presence or absence of 1 μM nucleozin. Influenza A NP accumulated in the nucleus at early infection stage and was distributed exclusively in the cytoplasm at late infection stage in the absence of nucleozin. At the indicated time point, cells were fixed and DAPI staining and mouse anti-influenza A NP antibodies were used to define the locations of the nucleus and viral NP respectively.



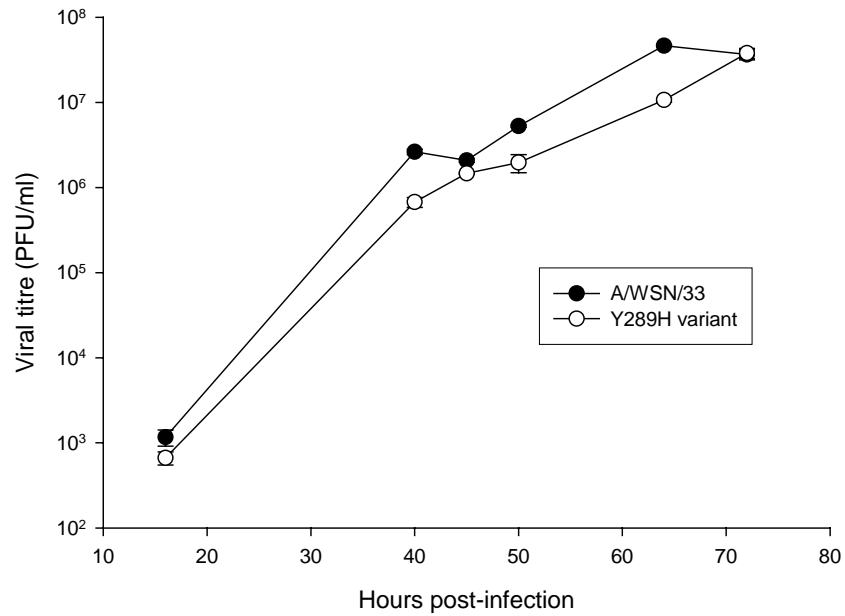
Supplementary Fig 4. Binding of nucleozin to the small groove in the back of the body of influenza A nucleoprotein. In this docking model, nucleozin is located in a small groove on the back of the body and interacts with residue N309 by hydrogen bond and Y289 by hydrophobic interaction, where the phenyl ring of compound is in parallel with the phenyl ring of Y289, and the distance between these two rings is between 3.2~4.3Å. (Sticks- grey: carbon, green: chlorine, blue: nitrogen, red: oxygen. Hydrogen bonds are denoted by yellow dash line).



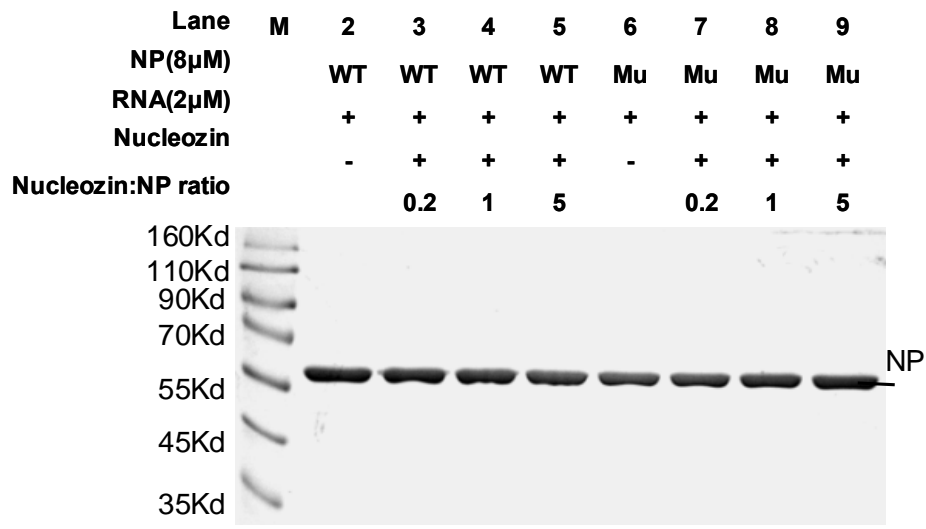
Supplementary Fig. 5. Binding of nucleozin to the RNA binding groove of influenza A nucleoprotein. In this docking model, nucleozin is located in the RNA binding domain, which spans the interior groove between body and head of the nucleoprotein, and nucleozin is interacting with residues Q364 and V363 that prohibit the RNA entering the arginine rich groove. Y148 was considered to be function as fixation of the first base of RNA. (Sticks- grey: carbon, green: chlorine, blue: nitrogen, red: oxygen. Hydrogen bonds are denoted by yellow dash line).



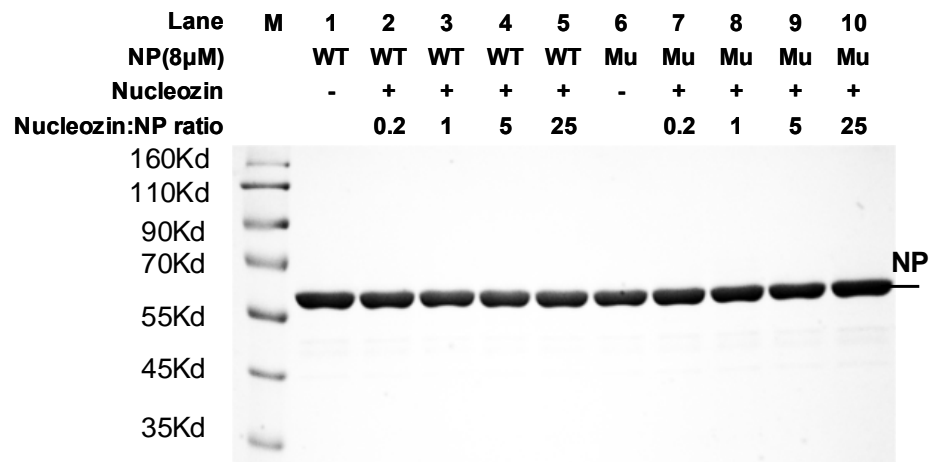
Supplementary Fig. 6. Binding of nucleozin to the tail loop groove of influenza A nucleoprotein. In this docking model, nucleozin is located in tail loop binding domain near to residue E339, and interacting with residues V186, R267, and G268 by hydrogen bonds. Nucleozin in this position breaks the salt bridge formed between E339 and R416 from another monomer. (Sticks- grey: carbon, green: chlorine, blue: nitrogen, red: oxygen. Hydrogen bonds are denoted by yellow dash line).



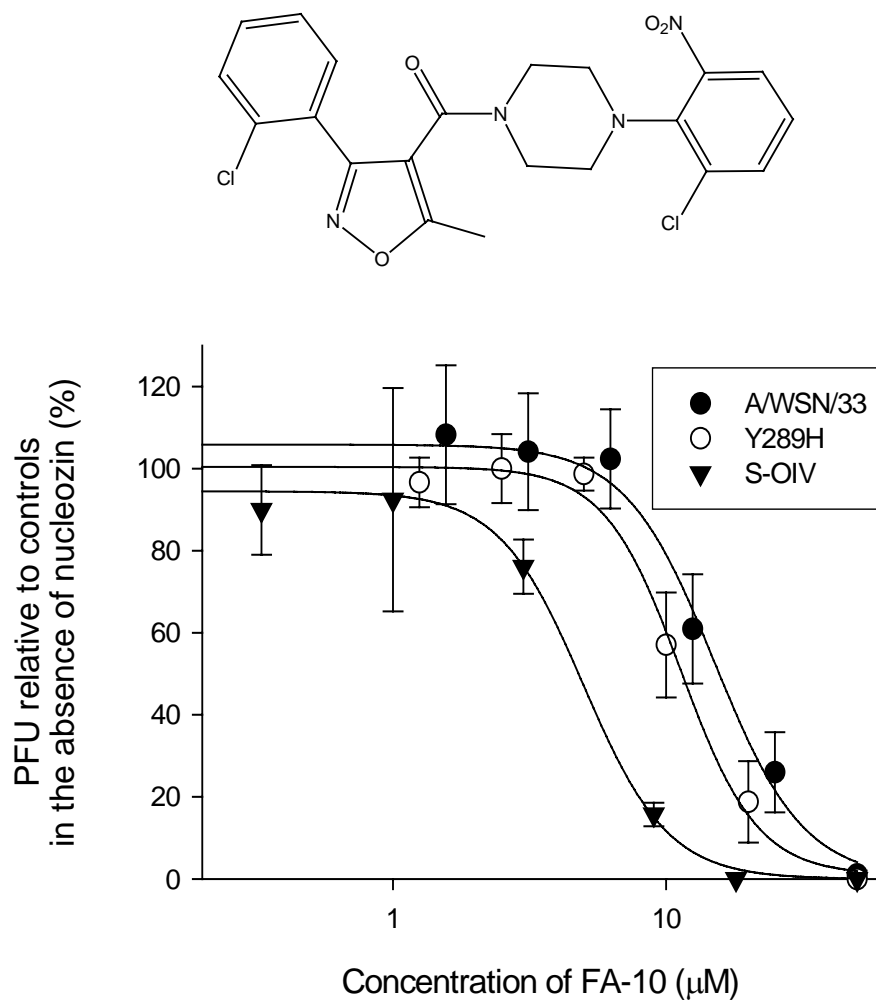
Supplementary Fig. 7. Comparison of viral titres obtained by the A/WSN/33 parental virus and the Y289H variant virus in MDCK cells. An MOI of 0.001 of each type of virus was used to infect MDCK cells. Viruses were harvested at the indicated time point and viral titres determined by plaque assay. The experiments were repeated twice for confirmation.



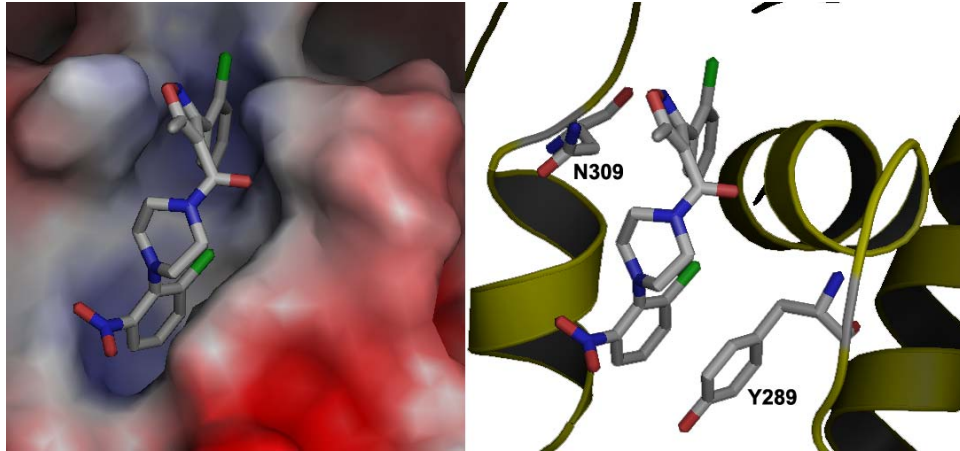
Supplementary Fig. 8. Denaturing SDS-PAGE of nucleozin-NP interaction assay reaction mixture (in the presence of RNA) under reducing conditions. A total of 2 μg of NP per lane was separated by denaturing SDS-PAGE under reducing conditions and NP subsequently visualized by Coomassie brilliant blue G-250 staining. M, protein molecular marker; WT, purified recombinant A/WSN/33 NP; Mu, purified recombinant Y289H variant NP; +, in the presence; -, in the absence. Position of NP is indicated.



Supplementary Fig. 9. Denaturing SDS-PAGE of nucleozin-NP interaction assay reaction mixture (in the absence of RNA) under reducing conditions. A total of 2 μg of NP per lane was separated by denaturing SDS-PAGE under reducing conditions and NP subsequently visualized by Coomassie brilliant blue G-250 staining. M, protein molecular marker; WT, purified recombinant A/WSN/33 NP; Mu, purified recombinant Y289H variant NP; +, in the presence; -, in the absence. Position of NP is indicated.



Supplementary Fig 10. The antiviral activities of compound FA-10, a close analogue of nucleozin, against WSN, Y289H variant, and swine-origin influenza A (H1N1) virus (S-OIV). MDCK cells were infected with different strains of virus and antiviral activities of compound FA-10 determined by PRA described in Methods. The chemical structure of compound FA-10 is also shown.



Supplementary Fig 11. Binding of FA-10 to the small groove in the back of the body of influenza A nucleoprotein. In this docking model, FA-10 binds favorably in binding site 1 of nucleozin (Supplementary Fig. 4). No hydrogen bond is found between FA-10 and residue N309 in this conformation. FA-10 is presumably stabilized largely by van der Waals force as the compound is buried deep in the groove and by hydrophobic interaction with the phenyl ring of Y289. (Sticks- grey: carbon, green: chlorine, blue: nitrogen, red: oxygen).

Supplementary table 1. Identification of NP Y289H variants in human influenza A subtypes. All available NP sequences deposited in GeneBank were analyzed.

Influenza A Subtype	Number of Y289H variant strains in NP gene
H1	525 / 1405
H2	0 / 92
H3	2 / 2199
H5	0 / 175
H7	0 / 4
H9	0 / 6

Supplementary table 2. Occurrence of Y289H variants in influenza A H1 subtype.

Year	Number of variants
1976	5
1988	5
1991	2
2005	1
2009	512 (swine-origin human H1N1)
<i>Total</i>	525

Supplementary table 3. Occurrence of Y289H variants in influenza A H3 subtype.

Year	Number of variants
2005	1
2007	1
<i>Total</i>	2

Supplementary reference

Zhang, J.H., Chung, T.D. & Oldenburg, K.R. A Simple Statistical Parameter for Use in Evaluation and Validation of High Throughput Screening Assays. *J Biomol Screen.* **4**, 67-73 (1999).